

Electronic structure of the valence band of II–VI wide band gap semiconductor interfaces

D. Olguín and R. Baquero

*Departamento de Física, Centro de Investigación y de Estudios Avanzados del IPN.,
Apartado Postal 14-740, 07000 México D.F.*

Abstract

In previous work we have discussed in detail the electronic band structure of a (001) oriented semi-infinite medium formed by some II–VI zinc blende semiconductor compounds in the valence band range of energy. Besides the known bulk bands (hh, lh and spin–orbit splitting), we found two characteristic surface resonances, one corresponding to the anion termination and another to the cation one. Furthermore, three (001)–surface–induced bulk states with no–dispersion from $\Gamma - X$ are also characteristic of these systems.

In this work we present the electronic band structure for (001)–CdTe interfaces with some other II–VI zinc blende semiconductors. We assume ideal interfaces. We use tight binding Hamiltonians with an orthogonal basis (sp^3s^*). We make use of the well-known Surface Green’s Function Matching method to calculate the interface band structure. In our calculation the dominion of the interface is constituted by four atomic layers. We consider here anion–anion interfaces only. We have included the non common either anion or cation (CdTe/ZnSe), common cation (CdTe/CdSe), and common anion (CdTe/ZnTe) cases. We have aligned the top of the the valence band at the whole interface dominion as the boundary condition.

The overall conclusion is that the interface is a very rich space where changes in the band structure with respect to the bulk do occur. This is true not only at interfaces with no common atoms but also at the ones with either common cation or anion atoms irrespective to the fact that the common atomic layers are facing or not each other at the interface.

Finally, we found that the (001)–surface–induced bulk states reappear at the interface in contrast to the pure (001)–surface resonances which disappear. This confirms our previous interpretation of such states as *bulk* states. Their behaviour is very interesting at the interface. We have refined the terminology for these states to update it to the new results and have called them *Frontier induced semi-infinite medium* (FISIM) states. They might well appear also in quantum wells and superlattices and have influence in the transport properties of these systems.

PACS: 73.61.Ga

I. INTRODUCTION

In the last ten years, the study of the physics of surfaces, interfaces, superlattices and quantum wells of semiconductors has been the object of permanent study.¹⁻⁹ At the origin of the deep understanding of the experimental results on these systems is an accurate description of its electronic band structures and its phonon spectra. In previous papers,⁹⁻¹⁶ in conjunction with the known surface Green's function matching method (SGFM)¹⁷, we have used a tight-binding formulation to calculate the electronic band structure, the surface, the surface induced, and the interface states for several systems in a consistent way with the known bulk band structure calculations. The method can also be applied to overlayers,¹⁸ superlattices,^{8,19} phonons²⁰ and to calculate transport properties²¹ in heterostructures as quantum wells, for example, by making use of the well known method by Keldysh.²²

Although there is no actual need to restrict ourselves to non-reconstructed ideal interfaces, we consider interesting to deal with this simpler situation. This is not a real limitation. Recent advances in thin film deposition technology²³ have allowed the fabrication of overlayers on surfaces, interfaces, and superlattices under stricter control of the parameters entering in the process of production, and samples with high degree of structural coherence are now possible. These artificially prepared materials are of great interest since they can exhibit properties different from those that occur in nature. Nevertheless, a minimum perfection in the growth of the samples is to be achieved before the properties manifest themselves. For example, superlattices will not exhibit their specific electronic properties unless interdiffusion between the two media is avoided to a great extent.²³

The semiconductor interfaces are less studied than their surfaces. Although interesting in themselves, the deep understanding of the physics of the interface is an important starting point for the detailed study of thermal, optical, photoacoustic and other properties of quantum-wells and superlattices. The electronic properties at solid-solid interfaces depend sometimes even on details of the interaction between the two atomic layers from the different materials in contact. Our work can be used as a starting point to analyze those details. These

are responsible for the characteristics of interface reconstruction, thermodynamic properties, degree of intermixing, stress, compound formation, etc.

In previous work,^{9,16} we have studied the electronic structure of the valence band for the (001)-surface of several II-VI wide band gap semiconductors. We have considered CdTe, ZnTe, CdSe and ZnSe. We have obtained the bulk bands (infinite medium) from the direct diagonalization of our tight-binding Hamiltonians and compared our results with the available data. The same result was obtained using the SGFM method, from the (001)-bulk-projected Green's function. This is actually a proof of consistency which gives us confidence in the new results. The main characteristics of the electronic spectra for these materials appear in Table I.

The general characteristic of the zinc blende II-VI wide band gap semiconductor valence band as we have obtained from our calculations is sketched in Fig. 1. The hh and lh bands follow each other closely in energy. The hh band disperses from Γ to X about 2.0 eV and the lh one about 2.4 eV. The spin-orbit splitting is about 1.0 eV in the Te-compounds and about 0.5 eV in the Se-ones. The spin-orbit band (SO) reaches X at about 5.0 eV. This is the band with the most dispersion. The LCAO composition is mainly (p_x, p_y) for the first two bands and (p_z) for the last one.

From the (001)-bulk-projected Green's function we get the energy of the (001)-surface-induced bulk states. Three such states appear, B_h , B_l and B_s , in this range of energy. These surface-induced bulk bands show no dispersion^{9,15,16} and were first found experimentally by Niles and Höchst⁴ and confirmed later by Gawlik *et al.*⁶ for CdTe(001). At X B_h mixes with the hh bulk band and B_l with the lh one. Both are of (p_x, p_y) -character. B_s mixes with the spin-orbit band at X and is mainly (s, p_z) . The three states appear at the same position in energy irrespective of the cation or anion termination of the surface as one expects for surface-induced *bulk* states which only depend on the surface through the boundary condition (the wave function has to be zero at the surface).

The (001)-surface valence band is very rich^{9,16} in several other features. In particular, two characteristic surface states do exist in this range of energy. One corresponds to the anion

(S_a) and the other to the cation (S_c) termination of the (001)-surface. In all the systems considered, the anion terminated surface band follows roughly the dispersion of the heavy hole bulk band but is at a slightly higher energy. The cation terminated surface band starts roughly around 2–3 eV from the top of the valence band in Γ and has a varying amount of dispersion. The two states appear at very different energy values and are distinctive of the termination of the surface for the four systems under consideration.

In this work, we want to extend these findings to the case of interfaces. We will study the valence band of several (001)-CdTe interfaces with other II–VI wide band gap zinc blende semiconductors, namely, (001)-CdSe, (001)-ZnTe and (001)-ZnSe. Our work can be straightforwardly extended to other interfaces using the data that we give in the appendix. Our paper is organized as follows. In section II, we summarize the method that we have used, section III is devoted to discuss our results and constitutes the main part of the paper. We describe in detail the valence band of the interfaces studied in this section. Section IV is devoted to the discussion of the frontier induced semi-infinite medium (FISIM) states which are reminiscent of the surface-induced bulk states. We then summarize our conclusions in a final section V.

II. METHOD

To describe the interface between two semiconductor compounds, we make use of tight-binding Hamiltonians. The Green's function matching method takes into account the perturbation caused by the surface or interface exactly, at least in principle, and we can use the bulk tight-binding parameters (TBP).^{10–12} This does not mean that we are using the same TBP for the surface, or for the interface and the bulk. Their difference is taken into account through the matching of the Green's functions. We use the method in the form cast by García-Moliner and Velasco.¹⁷ They make use of the transfer matrix approach first introduced by Falicov and Yndurain.²⁴ This approach became very useful due to the quickly converging algorithms of López-Sancho *et al.*²⁵ Following the suggestions of these authors,

the algorithms for all transfer matrices needed to deal with these systems can be found in a straightforward way.²⁶ This method has been employed successfully for the description of surfaces,^{9–11} interfaces,^{12,13} and superlattices.^{8,19}

A. The Formalism

We have calculated¹⁶ the bulk (infinite medium) band structure of the compounds by the tight-binding method (TB) in the Slater–Koster language²⁷ using an orthogonal basis of five orbitals, sp^3s^* . The s^* state is introduced to properly locate in energy the conduction band usually formed by d states in the II–VI zinc-blende (ZB) semiconductor compounds.^{28,29} We have included the effect of the spin–orbit (SO) interaction.³⁰ The TBP that we have used are listed in the Appendix. They reproduce the known bulk band structure calculations for all the semiconductors studied here.^{9,31,32}

To calculate the Green’s function for the interface, we first get the one for the free surface. We assume ideal truncation. The general equation for the Green’s function can be written as:

$$(\omega I - H)G = I, \quad (1)$$

where ω is the energy eigenvalue and I is the unit matrix. We adopt the customary description in terms of principal layers. Let $|n\rangle$ be the principal wave function describing the n^{th} principal layer. It is a LCAO wave function formed by one s -like, three p -like, and one s^* -like atomic wave function per spin per atom. Since there are two atomic layers in a principal layer, $|n\rangle$ is a 20-dimensional vector (2 spin states). If we take matrix elements of eq. (1) in the Hilbert space generated by the complete set of wave functions $|n\rangle$, we get

$$\langle n | (\omega I - H)G | m \rangle = \delta_{mn}. \quad (2)$$

Since, by definition, only nearest-neighbor interactions take place between principal layers, the identity operator to be introduced between $(\omega I - H)$ and G can be expressed as:

$$I = |n-1\rangle\langle n-1| + |n\rangle\langle n| + |n+1\rangle\langle n+1|. \quad (3)$$

By inserting (3) into (2) we get

$$(\omega - H_{nn})G_{nm} - H_{nn-1}G_{n-1m} - H_{nn+1}G_{n+1m} = \delta_{mn}. \quad (4)$$

This is because $H_{m,m+i} = 0$ for $i \geq 2$. The matrix elements of the Hamiltonian, H_{nm} , that appear in this formula are 2×2 supermatrices. For example, in the case of a surface

$$H_{00} = \begin{pmatrix} h_{00} & h_{0-1} \\ h_{-10} & h_{-1-1} \end{pmatrix}, \quad (5a)$$

$$H_{01} = \begin{pmatrix} h_{0-2} & h_{0-3} \\ h_{-1-2} & h_{-1-3} \end{pmatrix}. \quad (5b)$$

Notice that rows are labeled with the index of the surface principal layer zero (containing atomic layers 0 and -1 , for both H_{00} and H_{01}) while the columns are indexed with the zero and first principal layer (atomic layers 0 and -1 , and -2 and -3 , for H_{00} and H_{01} , respectively). We label principal layers with positive numbers and atomic layers with negative numbers. The surface is labeled with zero in both cases. We shall adopt the hypothesis of an ideal, non reconstructed surface. For the (001)-surface of a II-VI compound we have one atomic layer of anions and one of cations per principal layer. In this case $h_{00} \neq h_{-1-1}$ but $h_{0-1} = h_{-10}^\dagger$. To calculate H_{00} and H_{01} we only need to know h_{00} , h_{-1-1} , h_{0-1} , and h_{-1-2} , since $h_{0-2} = h_{0-3} = 0$ in the first nearest neighbors approximation. These matrices are readily written in the tight-binding language and can be calculated with *the bulk* TBP as mentioned above. All the h -matrices are functions of the wave vector \mathbf{k} .

Using (4) for $n = m$, and $m = 0$ for the surface, it is straightforward to get the surface Green's function¹⁷

$$G_s^{-1} = (\omega I - H_{00}) - H_{01}T \quad (6)$$

and the principal layer projected bulk Green's function¹⁷

$$G_b^{-1} = G_s^{-1} - H_{01}^\dagger \tilde{T}. \quad (7)$$

It is customary to define the transfer matrices as

$$G_{k+1p} = T G_{kp}, \quad k \geq p \geq 0 \quad (8a)$$

$$G_{ij+1} = \tilde{T} G_{ij}, \quad j \geq i \geq 0. \quad (8b)$$

These matrices can be calculated by the quick algorithm of López-Sancho *et al.*²⁵ (see also Refs. [11, 12, 26] for a compilation of the formulae and details of the algorithms used).

In the case of the interfaces the matrices double in size. The algebra is the same. One gets

$$G_I^{-1} = G_{s(A)}^{-1} + G_{s(B)}^{-1} - I_B H^i I_A - I_A H^i I_B, \quad (9)$$

which is the analogous formula to (6) above. G_I^{-1} is the interface Green's function, $G_{s(A)}^{-1}$ and $G_{s(B)}^{-1}$ are the surface Green's function of medium A and B, respectively, in the doubled space of the interface,

$$G_{s(A)}^{-1} = \begin{pmatrix} G_A^{-1} & 0 \\ 0 & 0 \end{pmatrix} \quad (10)$$

where G_A^{-1} is the surface Green's function for the medium A calculated from (6). It is a 20×20 matrix while G_I^{-1} is a 40×40 matrix. $I_B H^i I_A$ and $I_A H^i I_B$ are 40×40 matrices of the form

$$-I_B H^i I_A - I_A H^i I_B = \begin{pmatrix} 0 & -\mathcal{I}_A H^i \mathcal{I}_B \\ -\mathcal{I}_B H^i \mathcal{I}_A & 0 \end{pmatrix} \quad (11)$$

they describe the interaction between the two media. $-\mathcal{I}_A H^i \mathcal{I}_B$ and $-\mathcal{I}_B H^i \mathcal{I}_A$ are 20×20 matrices. In our model they take the form of the surface Hamiltonian H_{01} and H_{01}^\dagger , respectively, with TBP taken as the average of those for the two media. This is a reasonable approximation when both sides of the interface have the same crystallographic structure and we take the same basis of wave functions.

From the knowledge of the Green's function, the local density of states can be calculated from its imaginary part integrating over the two-dimensional first Brillouin zone. We have applied previously this formalism to surfaces^{10,11}, interfaces^{12,13} and superlattices¹⁹. Now we present our results.

III. RESULTS AND DISCUSSION

This section is devoted to the discussion of the interface valence band of the (001)-projected electronic band structure of II-VI zinc blende wide band gap semiconductors. We have calculated all the interfaces formed by CdTe, ZnTe, CdSe and ZnSe. In Table I we present the main characteristics of the band structure for these materials, as we already mentioned. We will present in this paper the CdTe-(001) interfaces in detail (see Figs. 2-4 and Table II) and we give all the necessary data so that the full electronic band structure for the rest of the interfaces can be reproduced, as experiments become available.

The domain of the interface is constituted by several atomic layers. Since we are considering first nearest neighbors interactions in our bulk Hamiltonians, we will consider four atomic layers as the interface domain, two belonging to medium A and two to medium B. To distinguish between the different atomic layers we will call each atomic layer by the medium its neighbors belong to. The atomic layer AA will be the second from the interface into medium A. AB will be the last atomic layer belonging to medium A and facing the first atomic layer of medium B and so on. So the four atomic layers that constitute the interface domain will be labeled AA, AB, BA, and BB. For the interfaces aligned along the (001) direction the two media are facing each other either through its anion or cation atomic layer. We will consider here the case of an anion-anion interface only. The notation (001)-CdTe/ZnSe means an interface constituted by two zinc blende crystals, CdTe and ZnSe, both aligned along the (001)-direction and where the atomic planes are identified as follows AA=Cd, AB=Te, BA=Se and BB=Zn. We will project the interface electronic band structure on each atomic layer and see how the different states that we found for the free

surface case change or disappear at the interface. New states, in principle, can appear at the interface. These interface states are important to know since they may play a role in the transport properties of heterostructures.

One important point is the band offset used. Experimental results for some II–VI semiconductors are available.^{7,33} In general, for II–VI semiconductors, the anion–anion interfaces have small valence band–offsets and cation–cation ones have small conduction band–offsets (both of the order of some meV). The rest of the bands and the surface–induced bulk states will show discontinuities accordingly. We will use the boundary condition that the top of the valence bands at the interface are aligned and choose this energy as our zero. As a consequence the conduction band offset will be equal to the difference in the band gaps. The surface-induced bulk states (see Table III) do survive at the interface; their energy position changes slightly and show dispersion in some cases contrary to the semi–infinite case (see Figs. 2–4 and Table IV). The interface builds up discontinuities characteristic of each one of them (see text below). The surface states do not survive and are not present at the interface domain, as expected. This gives further support to our interpretation of the –4.4 eV non–dispersive state⁹ found experimentally in CdTe–(001) by Niles and Höschel⁴ and by Gawlik *et al.*⁶ as a *bulk* state. We do not find interface resonances in this interval of energy.

In Figs. 2–4 and Tables II–IV, we show the electronic band structure of the valence band for the interfaces studied here, (001)–CdTe/ZnSe, (001)–CdTe/CdSe, and (001)–CdTe/ZnTe. The dispersion relations are found from the poles (symbols in the figures) of the real part of the interface Green’s function. The solid–lines are a guide to the eye. These are to be compared to the dispersion curves found for the bulk (infinite medium) case. As we mentioned above, the (001) surface-induced **bulk** states do survive as expected (stars, crosses and dots in Figs. 2–4). We should refine the convention for *surface-induced* bulk states as a result of these new findings and call them rather *frontier-induced semi-infinite medium* (FISIM) states to incorporate the interface case and probably other type of heterojunctions as well, and to introduce clearly the idea that they are semi–infinite medium states as opposed to bulk (infinite medium) or surface states. In the semi–infinite medium^{9,16} case

we have called these states B_h , B_l , and B_s according to the bulk band they mixed with at X in the First Brillouin zone. We now proceed to give a more detailed account for each particular interface studied.

A. The (001)-CdTe/ZnSe interface

Fig. 2 shows the electronic structure of the valence band (VB) for this interface. We consider an anion–anion (Te–Se) interface. As boundary condition we have aligned the top of the VB projected onto the atomic layer Te (AB) with the one projected onto the atomic layer Se (BA). We take this common energy value as our zero of energy. All the energies are in electron–volts (eV). The value of the top of the valence band projected onto the AA(Cd)– and BB(Zn)– atomic layer is for both also 0.0. There is a conduction band (CB) discontinuity at the interface of about 1.2 at the anion–anion interface (see Table I).

In Fig. 2a, we show the electronic band structure projected onto the Cd (AA) atomic layer. The full lines are the heavy hole (hh), light hole (lh) and the spin–orbit (SO) projected dispersion curves. They are actually a fit to the computed points which appear as empty triangles. In Table II, we summarize the main characteristics of the electronic dispersion curves for the interfaces under consideration. When compared to the bulk bands, the first difference with respect to the interface bands, is the larger width at the interface for each individual band although the total width for the three bands shown in the figure remains unchanged. The hh and lh band width in the bulk are 1.7 and 2.2 (see Table I), respectively, while at the AA(Cd) atomic layer at the interface are 2.1 and 2.3, respectively (see Table II). The degeneracy at this point is not broken by the interface. For the SO–shift in Γ the bulk and the surface band structure give both 0.95 (see Table I) in agreement with experiment. At the AA(Cd)–atomic layer of the interface, we find a smaller value, 0.6, as it is shown in Table II. This difference should be accessible to experimental verification. The SO–curve band width is again higher at the interface (3.8) than at the surface or in the bulk (3.5) as it is seen from a comparison of the corresponding values in Tables I and II. Nevertheless the

SO-curve projected onto the AA(Cd)-atomic plane reaches the X high-symmetry point of the Brillouin zone at -4.4 , and the total width of the three bands is the same in both cases (see Fig. 2a).

Another interesting aspect of the electronic band structure at the interface is the behaviour of the FISIM-states. We recall that the (001)-surface induces non-dispersion states^{4,6,9,16} in zinc blende II-VI semiconductors. In Figs. 2-4, the straight dotted lines are the dispersion curves found for the (001) surface case for the FISIM-states. These states do have dispersion at the interface domain as a consequence of the influence of the other crystal atoms instead of the vacuum existing at the surface frontier.

In Figs. 2, these states are labeled B_{Ih} , B_{Il} and B_{Is} , reminiscent of the corresponding notation used for the surface-induced ones (see also Table III). The dotted lines show the FISIM-states dispersion curves for the (001)-surface-induced states in the binary crystal case (CdTe or ZnSe). Fig. 2a (AA = Cd) shows that the B_{Ih} (stars) begins at -2.1 in Γ and ends in X at about -2.2 . As in the free (001)-surface case, this state is degenerate in Γ and bifurcates in two branches with an overall dispersion of about 0.5 . B_{Il} (crosses) shows less dispersion (-3.0 in Γ and -3.3 in X). The energy difference is 0.3 . In contrast B_{Is} (dots, at -4.7 and non degenerate as well) shows almost no dispersion. See Fig. 2a and Table IV. The energies at Γ and at X are, in general, slightly different from the corresponding ones in the (001)-surface case, see Table III. Fig. 2b shows the projection of the electronic band structure onto the (AB=) Te-atomic layer. A very similar analysis with analogous conclusions is made in this case. It is to be noticed that the FISIM-states show much more dispersion for this atomic layer projection than before. Also the overall width is larger than in the bulk case (see Table IV).

The other side of the interface is presented in Figs. 2c and 2d where the projection onto the Se- and Zn-atomic layer is shown, respectively. The top of the VB is fixed at 0.0 in the Se-projected dispersion relation. This constitutes the boundary condition. From Table I, we see that for ZnSe the bulk and the free (001) surface hh band takes the value of -1.95 at the X high-symmetry point. This value should be compared with -2.0 in the interface

region according to Figs. 2 and Table II. The lh state in the free (001) surface takes at X almost the same value for CdTe and ZnSe, namely -2.2 . The same value is found at the ZnSe side of the interface; see Tables I and II. A notable difference can be observed in the SO-band projected on the Zn-atomic layer. For this band we obtain the value of -4.8 at X at the interface domain which is quite less than the free (001)-surface value of -5.3 (see Table I).

From Table III we see that for the free ZnSe (001)-surface B_h is at -2.0 . The corresponding FISIM-state (see Fig. 2d) at the interface, B_{Ih} , shows a slight dispersion of about 0.5 in the $\Gamma - X$ region. B_l in the free (001)-surface is located roughly at -2.2 for both materials and at the interface (B_{Il}) it is at -2.4 . Finally, the B_{Is} state at the BA(Se) atomic layer projection of the interface follows roughly the non dispersive property of the corresponding (001)-surface FISIM state. The BB(Zn) projection shows a small dispersion.

In general, these FISIM-states are located at different energies in different materials and are either follow the non dispersive property of the (001)-surface ones or move to slightly deeper values in energy at the X high-symmetry point of the interface, as can be checked from Tables III and IV and from Figs. 2.

In conclusion, the VB of (001)-CdTe/ZnSe interface does present the overall features of the free (001)-surface ones but at energies that are slightly different. As it is expected the surface resonances do not appear at the interface. The FISIM-states do appear, a fact that is also expected since they are semi-infinite medium states. These states merge to deeper energies at this interface. They are mainly of $s - p$ anion states character. In Table V, we give the LCAO-composition for all the states that appear at the interfaces studied. The valence band offset used is zero.

B. The (001)-CdTe/CdSe interface

Here again, as we explained before, our notation means two zinc blende crystals aligned in the (001) direction forming an interface. In our previous notation AA=Cd, AB=Te,

BA=Se, and BB=Cd. The projected band structure is presented in Fig. 3. The symbols in the figure are obtained from the poles of the real part of the interface Green's function obtained within the SGFM formalism as before. The lines are interpolations meant as a guide to the eye. These should be compared to the bulk bands. The bulk band parameters of interest here for the two crystals forming the interface are quoted in Table I.

We consider an anion–anion (Te–Se) interface as before and the boundary condition is to align the top of the valence band in both sides of the interface. We take this common value as our zero of energy which we express again in eV. As it can be seen from Table I, the two crystals forming this interface have the smallest difference in their bulk gap value (0.18) in contrast with the previously studied (001)–CdTe/ZnSe where it is the highest (1.2). As a consequence of our used boundary condition this is the CB offset. This is therefore the interface with the smallest CB offset studied here.

The first thing to compare is the behaviour of the bands in the common medium A(CdTe) for the previous and this interface. In the AA(Cd) projection the hh band behaves very similar. It is only the value at the X –high symmetry point that differs by 0.3 (Table II and Figs. 2a and 3a). In contrast the lh bands develop differently in the sense that some points are at a higher distance in energy from the respective hh band ones in both graphs. In the AA(Cd) projection the lh band appears to be the more affected by the presence of a different partner at the interface. The SO-curve is again similar in both cases. The *Frontier-induced semi-infinite medium* (FISIM)–states associated with the lh and SO bands behave very similarly but, in contrast, the one associated with the hh bulk band differs for the AA(Cd) projection at the two interfaces.

The anion AB(Te) atomic layer projected bands do differ but slightly for the two interfaces.

Next, it is interesting to compare the behaviour of the AA(Cd) projected bands with the BB(Cd) ones for this (001)–CdTe(A)/CdSe(B) anion–anion interface. The hh and lh curves for the BB(Cd) projected bands at this interface (Fig. 3d) behave very similar to the AA(Cd) (Fig. 2a) ones for the (001)–CdTe/ZnSe interface but the SO curves do not. The

FISIM-states do differ in the way they disperse and in the energy position value.

This common-cation anion-anion interface presents also the interesting feature that the spin-orbit shift is different at the AB(Te) and BA(Se) atomic layer projections (0.8 and 0.9, see Table II and Figs. 3b, and 3c) than at the AA(Cd) and BB(Cd) projections (0.5, Table II and Figs. 3a and 3d).

In conclusion, the band structure for this interface shows that the very same atomic layer not facing directly the other medium at the interface can present noticeably differences in the projected band structure in different interfaces and in different sides of the same interface. This introduces more subtleties into the complicated problem of the calculation of the band offsets.

C. The (001)-CdTe/ZnTe interface

This is a different case, the common-anion anion-anion interface. We use again the same boundary condition for the VBs. The CB offset is then equal to the difference between the bulk band gaps. One interesting point in this case is to compare the AB(Te) and BA(Te) projected band structures (See Figs. 4b and 4c and Tables II and IV). Another point of interest is to compare the behaviour of the band structure at the BB(Zn) atomic layer for this interface with the BB(Zn) for the (001)-CdTe/ZnSe interface studied previously (See Figs. 2d and 4d and Tables II and IV). The analysis is very similar to the one made above and leads to the new conclusion that the same atomic layer (Te) facing each other at an interface can show characteristics of the band structure that are different.

IV. THE FISIM-STATES

The *Frontier Induced Semi-Infinite Medium* (FISIM)-states were reported experimentally by Niles and Höchst⁴ and confirmed later on by Gawlik *et al.*⁶ in the (001)-CdTe oriented semi-infinite crystals. We succeeded in showing where these states come from.^{9,16} We have reproduce their energy position and non-dispersive character from the poles of the

real part of the semi-infinite medium Green's function. We showed that these states are of *semi-infinite medium (bulk)* character as opposed to *surface* character. The fact that no surface resonances survive at the interface but the FISIM-states do, confirms our interpretation. The FISIM-states have some dispersion at the interface domain and it is to be assumed that the second medium is responsible for the changes in the dispersion properties of these states. It is to be expected from quantum mechanics that given a Hamiltonian the changes in the boundary conditions from infinite-medium to semi-infinite do manifest themselves in changes of some of the properties of the eigenfunctions in both cases. The semi-infinite medium wave function losses in a certain direction the periodic condition. This is essentially the origin of the FISIM states.

V. CONCLUSIONS

We have presented the results for three of a series of band structure calculations for interfaces formed by II-VI wide band gap zinc blende semiconductors. We have included the non common either anion or cation, common cation and common anion cases. All our interfaces are anion-anion ones. The boundary condition used was to align the top of the valence bands at the interface domain. In our approximation it amounts to four atomic layers altogether. We have used the known SGFM method to calculate the interface Green's function and have produced the projected band structure at each atomic layer of the interface. We have used tight-binding Hamiltonians to describe the two media. Our parameters give very reasonable bulk band structures that agree with the known experimental data for the II-VI wide band gap semiconductors that we have been concerned with in this work. The parameters are given in the Appendix so that these and other results can be reproduced by the interested reader. We recall that the input to SGFM method are the bulk parameters. This does not mean that the same parameters are used for the surface or the interface and the bulk. The difference is taken into account by the method itself. To describe the interaction at the interface we have used linear combination of the tight-binding parameters

for the two media.

The overall conclusion is that the interface is a very rich space where changes in the band structure with respect to the bulk do occur. This is true not only at interfaces with no common atoms but also at the ones with either common cation or anion atoms irrespective to the fact that the common atomic layer are facing or not each other at the interface. This introduces further subtleties to the complicated problem of the calculation of the band offset.

A very interesting point is the behaviour of the *Frontier Induced Semi Infinite Medium* (FISIM)–states. In this work we showed that no surface resonances survive at an interface but, in contrast, the FISIM–states do. This confirms the interpretation that we gave before about these states in the sense that these are not surface states. The FISIM–states have no dispersion at a semi-infinite medium with a free surface but show some at an interface (see Figs 2–4 and Table IV). Their LCAO–composition is shown in Table V for completeness.

All these details of the interface band structure should manifest in the transport properties of heterojunctions and should influence the behaviour of a device. In this concern it will be interesting to study the the band structure of ternary and quaternary compounds interfaces, quantum wells and superlattices.

REFERENCES

- ¹ G. W. Bryant, Phys. Rev. Lett. **55**, 1786 (1985)
- ² J. E. Lowther, J. Phys. C: Solid State Phys. **19**, 1863 (1986)
- ³ D. G. Kilday, G. Maragaritondo, T. F. Ciszek, and S. K. Deb, J. Vac. Sci. Technol. B **6**, 1364 (1988) **19**, 1863 (1986)
- ⁴ D. Niles and H. Höchst, Phys. Rev. B **43**, 1492 (1991)
- ⁵ W. Bala, M. Drozdowski, and M. Kozielski, Acta Physica Polonica A **80**, 723 (1991)
- ⁶ K. –U. Gawlik, J. Brüggmann, S. Harm, C. Janowitz, R. Manzke, M. Skibowski, C. –H. Solterbeck, W. Schattke, and B. A. Orlowski, Acta Physica Polonica A **82**, 355 (1992)
- ⁷ T. M. Duc, C. Hsu, and J. P. Faurie, Phys. Rev. Lett. **58**, 1127 (1987)
- ⁸ J. Arriaga and V. R. Velasco, Phys. Scripta **46**, 83 (1992)
- ⁹ D. Olguín and R. Baquero, Phys. Rev. B **50**, 1980 (1994)
- ¹⁰ R. Baquero, V. R. Velasco, and F. García–Moliner, Physica Scripta **38**, 742 (1988)
- ¹¹ R. Baquero and A. Noguera, Rev. Mex. Fís. **35**, 638 (1989)
- ¹² C. Quintanar, R. Baquero, V. R. Velasco and F. García–Moliner, Rev. Mex. Fís. **37**, 503 (1991).
- ¹³ R. Baquero, A. Noguera, A. Camacho, and L. Quiroga, Phys. Rev. B **42**, 7006 (1990)
- ¹⁴ F. Rodríguez, A. Camacho, L. Quiroga, and R. Baquero, Phys. Status Solidi B **160**, 127 (1990)
- ¹⁵ D. Olguín, M. Sc. Thesis, CINVESTAV-IPN, México 1994.
- ¹⁶ D. Olguín and R. Baquero, Phys. Rev. B **51**, 16981 (1995).
- ¹⁷ F. García–Moliner and V. R. Velasco, Prog. Surf. Scie. **21**, 93 (1986)

- ¹⁸ R. Baquero, M. Yañez, and M. Salmerón, J. Phys. (Condens. Matter) **5**, A161 (1993).
- ¹⁹ V. R. Velasco, R. Baquero, R. A. Brito-Orta, and F. García-Moliner, Condens. Matter **1**, 6413 (1989)
- ²⁰ R. A. Brito-Orta, V. R. Velasco, and F. García-Moliner, Phys. Scripta **37**, 131 (1988); Phys. Rev. B **38**, 9631 (1988)
- ²¹ A. Camacho, D. Olgún and R. Baquero, Rev. Col. Fís. **27**, 611 (1995).
- ²² L. V. Keldysh, Zh. Eksp. Teor. Fiz. **47**, 1515 (1965) [Sov. Phys. JETP. **20**, 1018 (1965)]
- ²³ C. M. Falco and I. K. Schuller, in *Synthetic Modulated Structures*, edited by L. L. Chang and B. C. Giessen (Academic, New York 1985)
- ²⁴ L. Falicov and F. Yndurain, J. Phys. C: Solid St. Phys. **8**, 147 (1975)
- ²⁵ M. P. López-Sancho, J. M. López-Sancho, and J. Rubio, J. Phys. F: Metal Phys. **14**, 1205 (1984); **15**, 855 (185)
- ²⁶ R. Baquero, unpublished
- ²⁷ J. C. Slater and G. F. Koster, Phys. Rev. **94**, 1498 (1954)
- ²⁸ P. Volg, H. P. Hjalmarson, and J. D. Dow, J. Phys. Chem. Solids **14**, 365 (1983)
- ²⁹ W. A. Harrison, Phys. Rev. B **24**, 5835 (1981)
- ³⁰ D. J. Chadi, Phys. Rev. B **16**, 790 (1977)
- ³¹ D. Bertho, D. Boiron, A. Simon, C. Jouanin, and C. Priester, Phys. Rev. B **44**, 6118 (1991)
- ³² A. Camacho, private communication.
- ³³ K. Pelhos, S. A. Lee, and Y. Rajakarunanayake, Phys. Rev. B **51**, 13 256 (1995); Y. Rajakarunanayake, R. H. Miles, G. Y. Wu, and T. C. McGill, Phys. Rev. B **37**, 10 212

(1988)

FIGURES

FIG. 1. The general characteristic of the zinc blende wide band gap semiconductor electronic valence band structure. We show the heavy hole (hh), light hole (lh), spin-orbit (SO), and the lower s -cation character (b_{10}) bulk bands. Furthermore, we have the bulk surface-induced states B_h , B_l , and B_s (the FISIM states, see text) and the surface resonances S_{a1} , S_{a2} , and S_c . For details see Ref. [16].

FIG. 2. The full electronic valence band structure for (001)–CdTe/ZnSe interface in the $\Gamma - X$ direction. The dispersion relations (triangles) are found from the poles of the real part of the interface Green's function. The solid lines are a guide to the eye. The FISIM-states are shown as stars, crosses and points. The dotted lines show the FISIM-states (see text) for the (001)–surfaces in the binary crystal (from Ref. [16]).

FIG. 3. Electronic valence band structure of the (001)–CdTe/CdSe interface. The conventions are the same as in Fig. 2 (see figure caption).

FIG. 4. Electronic valence band structure of the (001)–CdTe/ZnTe interface. See figure caption 2 for details.

TABLES

TABLE I. Characteristic values taken from the bulk electronic band structure for the four binary II–VI compounds of interest in this work. The origin is at the top of the valence band and the energies are given in eV. The columns give the gap (Γ_6^c), the spin–orbit splitting (Γ_7^v), the value of the heavy hole dispersion curve at the X point (X_7^v), the light–hole one (X_6^v) and the spin–orbit one (X_6^v).

	Γ_6^c	Γ_7^v	X_7^v	X_6^v	X_6^v
CdTe	1.602	−0.9	−1.7	−2.2	−4.4
CdSe	1.78	−0.4	−2.18	−2.36	−4.89
ZnTe	2.39	−0.91	−1.93	−2.40	−5.50
ZnSe	2.82	−0.45	−1.95	−2.19	−5.30

TABLE II. Energies for the heavy hole (hh), light hole (lh), and spin-orbit (SO) bands at Γ and X high-symmetry points as obtained for the interface domain for (001)–CdTe/ZnSe, (001)–CdTe/CdSe, and (001)–CdTe/ZnTe. The energies are in eV.

		Γ -point	X -point		
System	Atomic layer	E_{so}	E_{hh}	E_{lh}	E_{so}
CdTe / ZnSe	Cd	−0.6	−2.1	−2.3	−4.4
	Te	−0.6	−2.0	−2.4	−4.8
	Se	−0.6	−2.0	−2.2	−5.2
	Zn	−0.6	−2.0	−2.2	−4.8
CdTe / CdSe	Cd	−0.5	−2.4	−2.5	−4.3
	Te	−0.8	−2.2	−2.3	−4.7
	Se	−0.9	−2.3	−2.6	−4.9
	Cd	−0.5	−2.2	−2.4	−4.9
CdTe / ZnTe	Cd	−1.0	−2.0	−2.3	−4.3
	Te	−0.8	−1.7	−1.9	−4.5
	Te	−1.0	−1.9	−2.1	−5.6
	Zn	−1.0	−1.9	−2.1	−4.8

TABLE III. Energies for the FISIM states (see text) for the free (001)–surface. Values taken from Ref. [16].

State	CdTe	CdSe	ZnTe	ZnSe
B_h	−1.8	−2.2	−2.0	−2.0
B_l	−2.2	−2.45	−2.5	−2.3
B_s	−4.4	−5.0	−5.5	−5.3

TABLE IV. Energies for the FISIM states (see text), B_{Ih} , B_{Il} , and B_{Is} , at the interface dominion of (001)–CdTe/ZnSe, (001)–CdTe/CdSe, and (001)–CdTe/ZnTe.

		Γ -point			X -point		
System	Atomic layer	B_{Ih}	B_{Il}	B_{Is}	B_{Ih}	B_{Il}	B_{Is}
CdTe/ZnSe	Cd	−2.1	−3.0	−4.7	−2.2	−3.3	−4.8
	Te	−1.5	−2.5	−4.8	−2.4	−2.6	−4.8
	Se	−1.5	−2.4	−5.2	−2.2	−2.5	−5.4
	Zn	−1.9	−2.4	−5.2	−2.2	−2.5	−5.4
CdTe/CdSe	Cd	−2.5	−2.9	−4.6	−2.5	−3.2	−4.8
	Te	−2.4	−2.8	−4.8	−2.4	−3.0	−4.7
	Se	−1.9	−2.5	−5.0	−2.3	−2.6	−5.1
	Cd	−2.0	−2.5	−4.9	−2.4	−2.6	−5.1
CdTe/ZnTe	Cd	−2.0	−2.9	−4.5	−2.3	−3.2	−4.8
	Te	−1.8	−2.7	−4.7	−2.3	−2.7	−4.5
	Te	−2.0	−2.5	−5.8	−2.4	−2.6	−5.9
	Zn	−1.9	−2.4	−5.8	−2.1	−2.8	−5.8

TABLE V. LCAO composition of the wave function for the states existing at the interface dominion in all the examples considered in this work.

State	Composition
hh	(p_x, p_y)
lh	(p_x, p_y)
so	(p_z)
B_{Ih}	(p_x, p_y)
B_{Il}	(p_x, p_y)
B_{Is}	(s, p_z)

APPENDIX:

TABLE VI. Tight-binding parameters used in our calculation. We used the notation of Bertho *et al.* Ref. [31]

Parameter	CdTe ^a	ZnTe ^b	ZnSe ^b	CdSe ^c
E_s^a	-8.1921	-9.19000	-12.42728	-10.16740
E_p^a	0.3279	0.62682	1.78236	1.03400
E_s^c	-0.95	-1.42	0.04728	1.07977
E_p^c	6.9379	3.77952	5.52031	7.64650
V_{ss}	-5.0000	-6.64227	-6.50203	-2.89240
V_{xx}	2.13600	1.94039	3.30861	3.01320
V_{xy}	5.28170	4.07748	5.41204	5.73040
V_{sp}^{ac}	3.31200	5.92472	1.13681	2.16040
V_{sp}^{ca}	3.63824	4.67265	5.80232	5.65560
$E_{s^*}^a$	10.44540	6.22682	7.84986	6.02650
$E_{s^*}^c$	6.62960	6.77952	8.52031	3.96150
$V_{s^*p}^{ac}$	2.52468	2.96202	3.26633	2.11640
$V_{s^*p}^{ca}$	2.94540	3.82679	1.86997	2.21680
λ_a	0.32267	0.36226	0.19373	0.14300
λ_c	0.07567	0.02717	0.01937	0.06700

^a Reference [9]

^b Reference [31]

^c Reference [32]

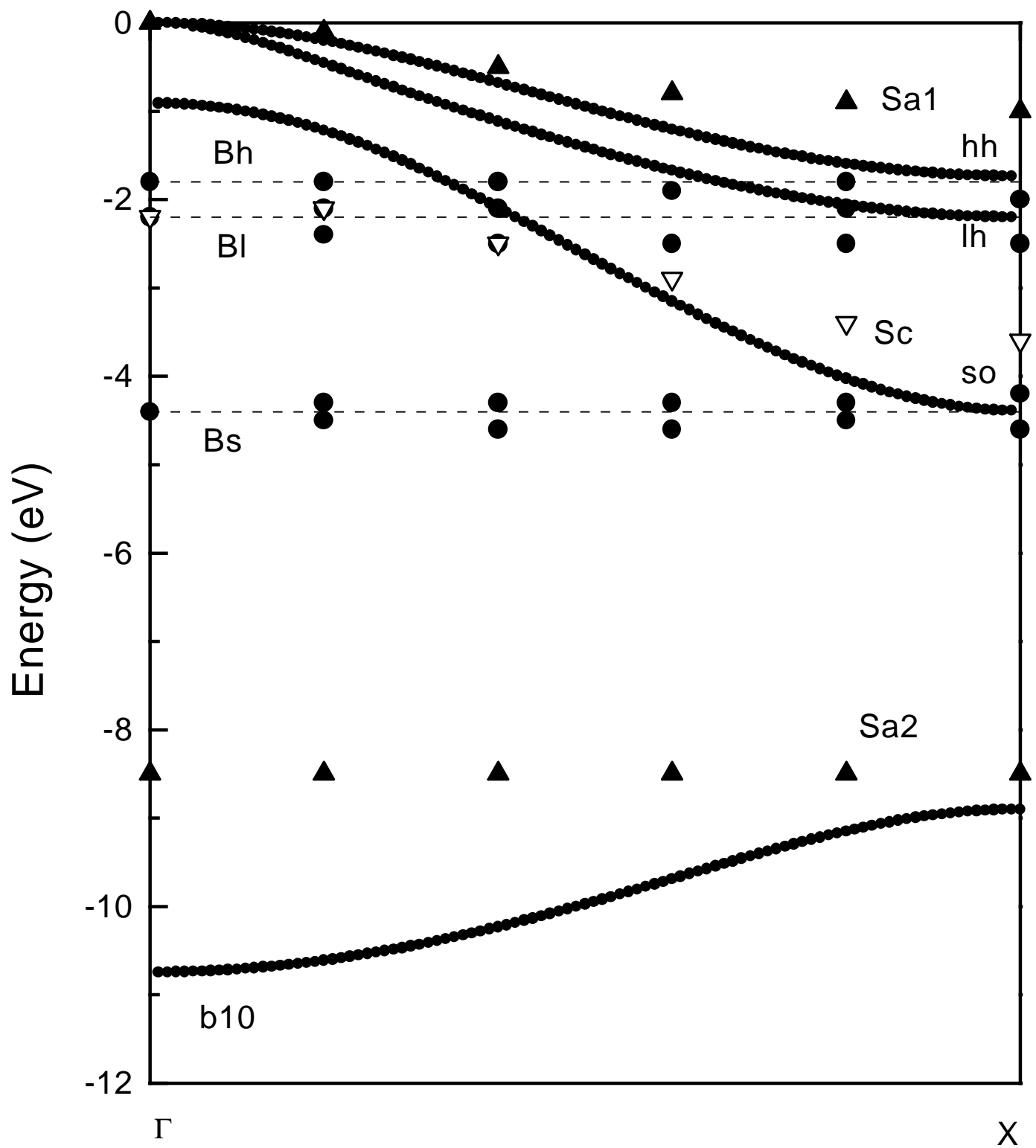


Fig. 1 Olguin & Baquero, PRB 15

(001)-CdTe/ZnSe

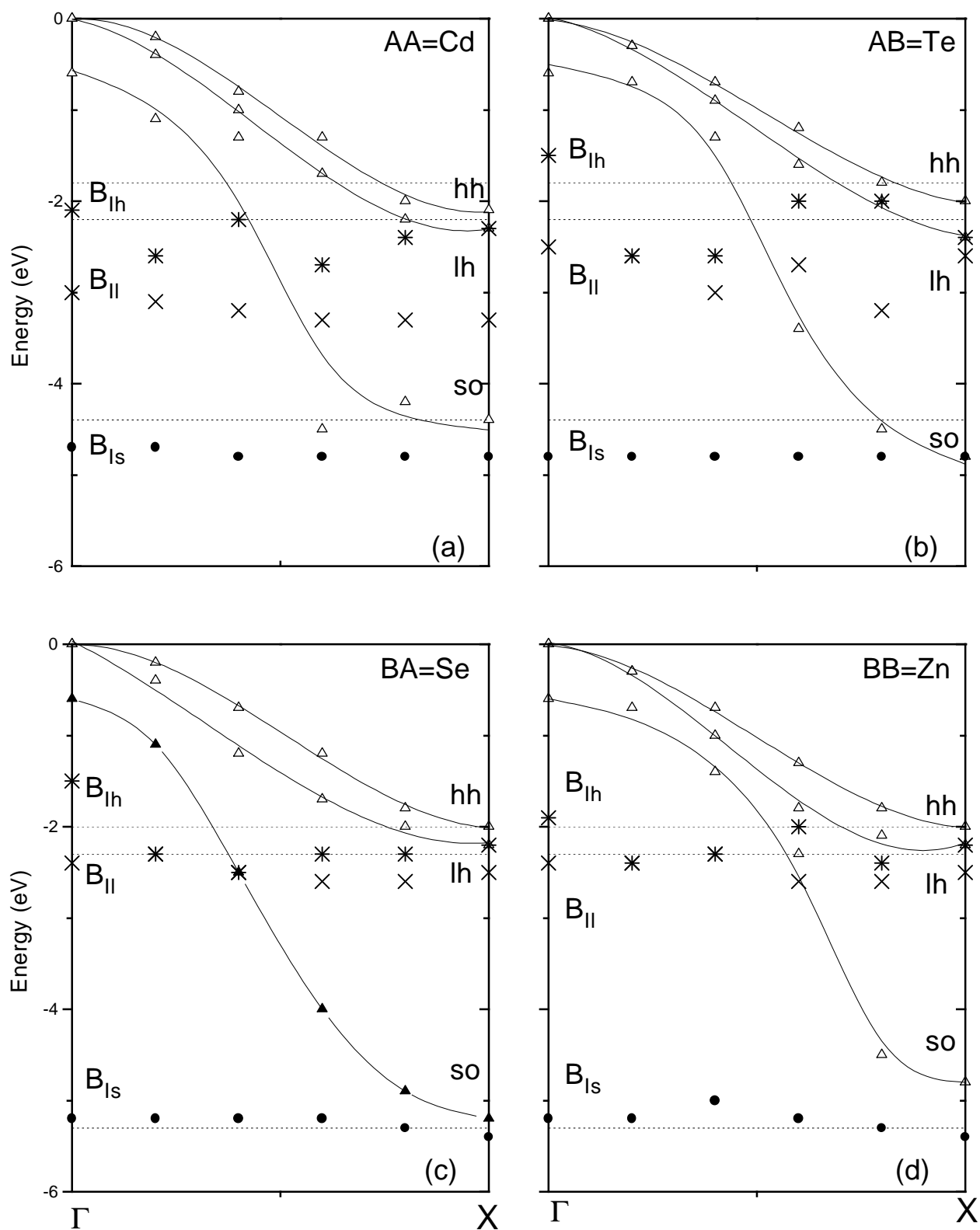


Fig. 2 Olguin & Baquero, PRB 15

(001)-CdTe/CdSe

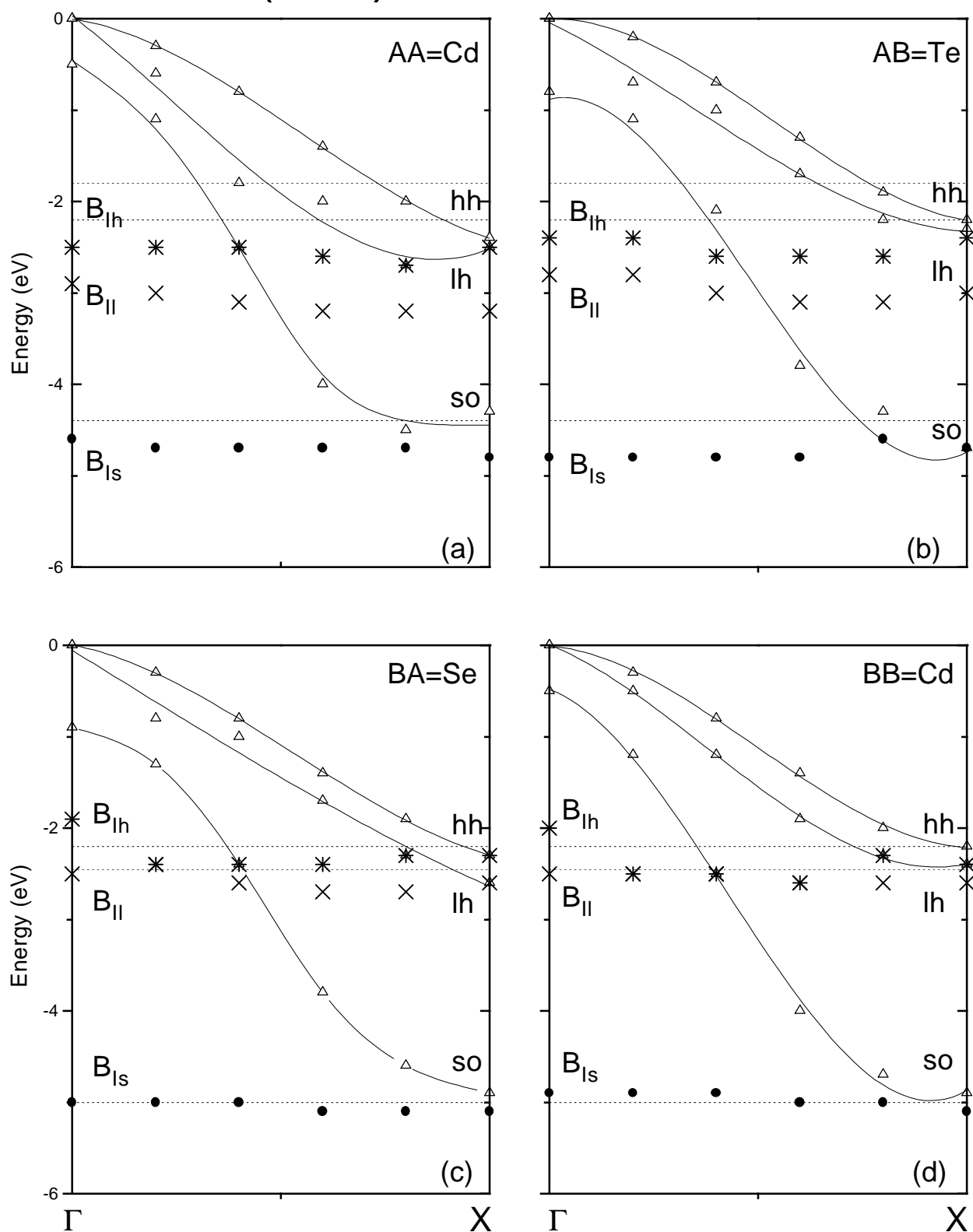


Fig. 3 Olguin & Baquero, PRB 15

(001)-CdTe/ZnTe

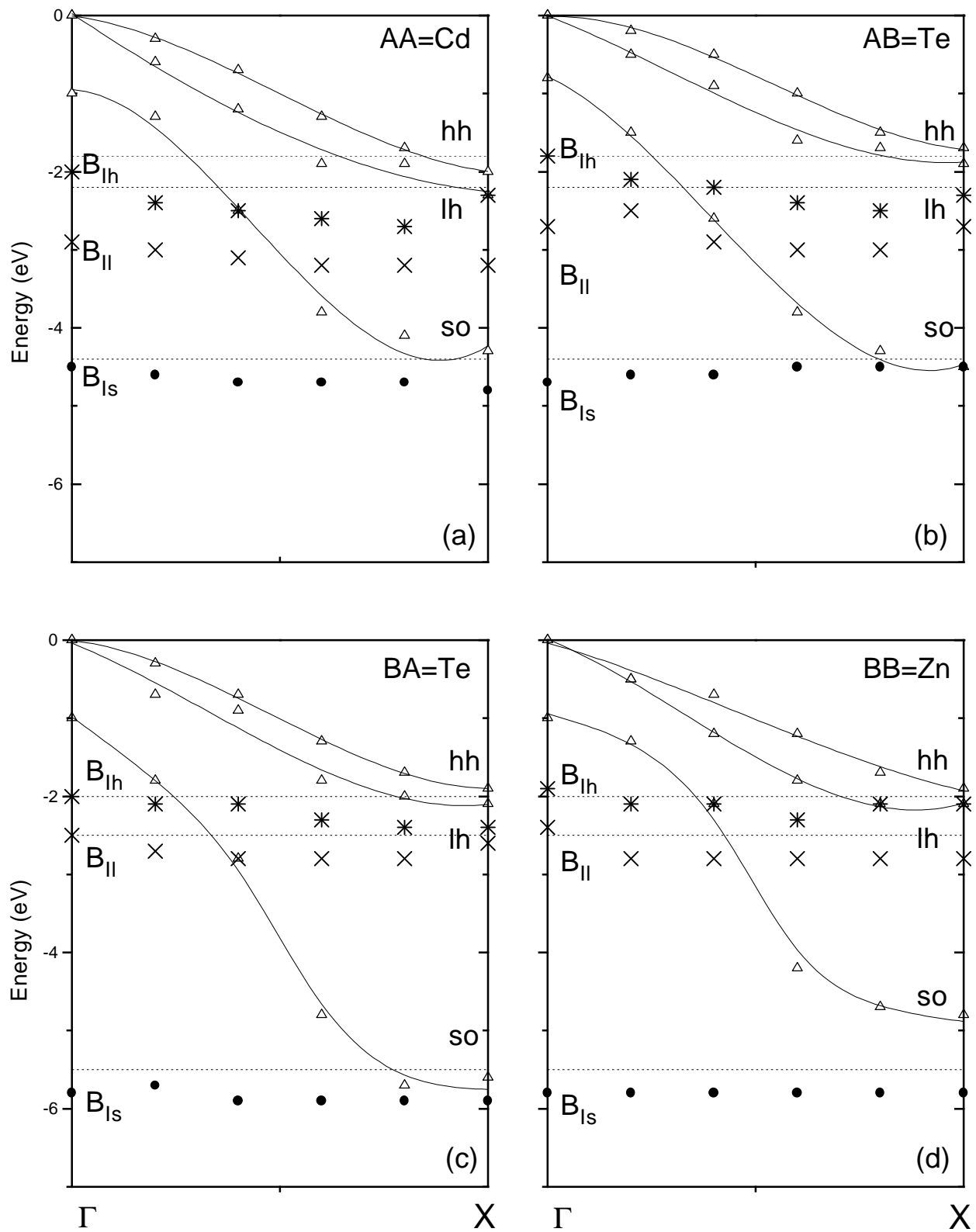


Fig. 4 Olguin & Baquero, PRB 15